# Hubble Space Telescope Precision Pointing Control System

G. A. Beals,* R. C. Crum,† H. J. Dougherty,‡ D. K. Hegel†, J. L. Kelley§, and J. J. Rodden¶
*Lockheed Missiles & Space Co., Inc., Sunnyvale, California*

**The Hubble Space Telescope has the most stringent pointing requirements imposed on any spacecraft to date. The overall HST pointing stability shall be 0.007 arcsec rms or less. The Pointing Control System uses fine-guidance sensors and rate gyros for attitude reference and rate information. Control torques are provided by reaction wheels. A digital computer collects the sensor data, performs the control law computations, and sends torque commands to the reaction wheels. To attain this precision pointing, improvements were made to the rate gyros to lower their noise characteristics and to the reaction wheels to reduce their induced vibration levels. The control system design was validated in a test sequence that progressed from model verification tests on an air-bearing to operations-oriented, closed-loop testing on the assembled vehicle. A test system is described that allowed the simultaneous production of test-case command loads for the flight computer and plots of predicted profiles to assist in test data analysis. Testing and analysis indicated that the HST will be capable of meeting the requirements for precision pointing.**

## Nomenclature

FGS = Fine-Guidance Sensor
FHST = Fixed-Head Star Tracker
FOV = Field of View
HSIF = Hardware/Software Integration Facility
HST = Hubble Space Telescope
PCS = Pointing Control System

## Introduction

THE NASA Hubble Space Telescope (HST), shown in Fig. 1, is a 2.4-m free-flying telescope designed to allow scientists to observe the universe with a clarity and range never before achieved. The HST performance requires stabilizing the telescope to a fine-pointing stability of 0.007 arcsec to allow near-diffraction limited images to be obtained. The space-based observatory maintains this stability both for stellar observations of up to 24 h and during the precision tracking of solar objects. The telescope must also provide the ability to return to a target with an accuracy of 0.01 arcsec or better. In addition to these fine-pointing requirements, the HST Pointing Control System (PCS)[1,2] provides the capability to maneuver the telescope 90 deg in 20 min or less.

The PCS objectives are met using precision sensors and actuators. Rate gyro assemblies provide rate information that is supplemented by attitude data from a user-selectable combination of NASA-standard fixed-head star trackers (FHSTs) and fine-guidance sensors (FGSs). The FGSs use photomultiplier tubes in an interferometric mode to provide a precision attitude reference. Actuation is accomplished by reaction wheel assemblies sized to provide both the torque needed for maneuvering and the precision-control torques required during fine pointing. Magnetic torquers are used for momentum management.

The flight digital computer performs computations for the control law, attitude reference, momentum management law, and the command generator, as illustrated in Fig. 2. The PCS control law incorporates a finite-impulse response filter in the rate path to provide an adequate stability margin with respect to the spacecraft structural modes. The position path uses an attitude observer to combine the attitude data derived from the FGS or star trackers with the rate data from the gyros. Momentum management processing uses magnetometers and magnetic torquers to minimize the reaction wheel speeds. The command generator shapes the acceleration feedforward commands to the control system in order to limit structural mode excitation. All commands requiring motion of the vehicle and FGSs are processed through the command generator to ensure adequate "smoothing" of the motion to meet fine-pointing requirements.

The PCS provides the capability of autonomous maneuvering, star acquisition, and fine pointing based on time-tagged stored program commands, as well as the ability to accept realtime interactive commands from the Space Telescope Operations Control Center. The capabilities of the HST PCS will support the data gathering of five scientific instruments including cameras, spectrographs, and a photometer. This paper will describe how the elements of the PCS work together to provide the precision-pointing control required for this scientific mission. Improvements to some of these elements will be discussed and system-level test results will be presented.

## Primary Control System

The precision-pointing reference is obtained from the FGSs. Three FGSs share the telescope field of view, shown in Fig. 3, with the scientific instruments. Each FGS has a field of view of about 60 square arcmin. Four photomultiplier tubes are used for both acquisition and fine pointing. For fine pointing, the output of the tubes is differenced for use in an interferometric mode. Because of the limited dynamic range of the interferometer (approximately ±0.02 arcsec), the FGS uses the sum output of the photomultiplier tubes to achieve initial star acquisition after the PCS maneuvers the telescope from one target star to another. The FGS contains star selectors, which are rate-control servos with rotating prisms, to allow the five-square-arcsec instantaneous FOV to be maneuvered over the total 60-square-arcmin FOV of the FGS. The various operational modes of the FGS allow the sensor to acquire a

Received Aug. 8, 1986; presented as Paper 86-1981 at the AIAA Guidance, Navigation and Control Conference, Williamsburg, VA, Aug. 18-20, 1986; revision received May 4, 1987. 

*Senior Research Engineer, Guidance, Navigation, and Control Systems. Member AIAA.
†Senior Associate Engineer, Guidance, Navigation, and Control Systems. Member AIAA.
‡Technical Consultant, Hubble Space Telescope. Member AIAA.
§Staff Engineer, Pointing Control System, Hubble Space Telescope.
¶Program Engineering Manager, Astronautics Division. Member AIAA.

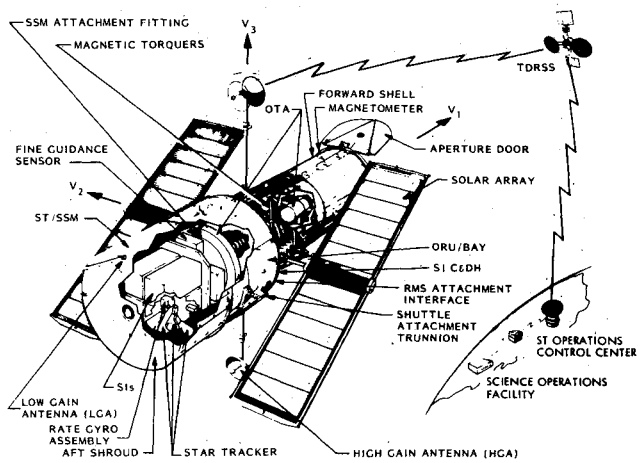


**Fig. 1 Hubble Space Telescope System.**

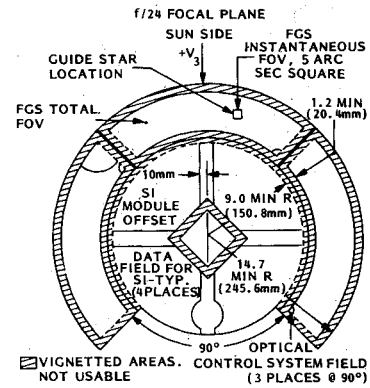


**Fig. 2 Pointing Control System block diagram.**

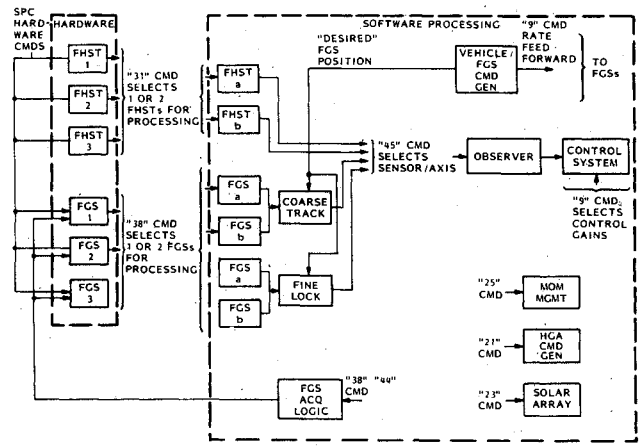


**Fig. 3 Optical telescope assembly focal plane.**

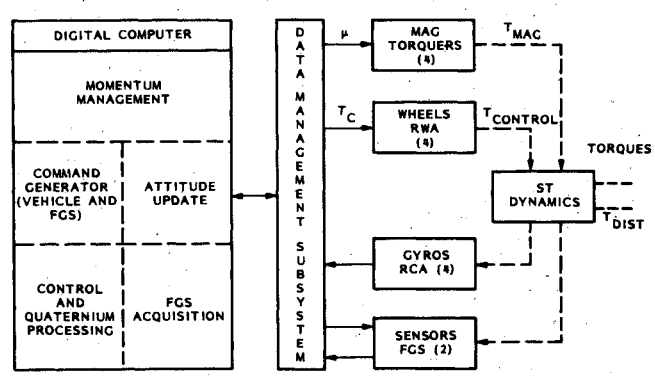


**Fig. 4 Overview of user control of hardware/software interface.**

star with a position uncertainty of 90 arcsec and provide accuracy on the order of milliarcseconds.

Of the three FGSs, two are used by the PCS for control during stellar pointing or solar object tracking. The third is available for use as a scientific instrument in its astrometry mode. The rate gyros are used for rate and short-term attitude information. One of the FGSs is used for the attitude correction of the telescope line of sight. Information from both FGSs is used to provide attitude corrections about the line of sight.

Rate measurement is provided by four of six available rate-integrating gyros configured in quantized, pulse width-modulated, rebalance loops. The rate gyros are paired in three sensor units containing two gyro channels each. The gyros have a dual rate range: the high-rate scale range is 0.5 deg/s with a pulse weight of 0.0075 arcsec, and the low-rate scale range is 20 arcsec/s with a 0.000125-arcsec pulse weight.

Four reaction wheel assemblies generate control torques. The torque-producing axes of the reaction wheels are skewed relative to the HST coordinate frame to provide system redundancy. Thus, the PCS can operate with only three reaction wheels. Each reaction wheel has 0.8-N/m output torque capability, 3,000-rpm maximum speed, and 0.84-kg/m$^2$ rotor inertia.

Essentially all PCS capabilities are available for user access and configuration during scientific operations[3] via user-defined command packets. An overview of the user control of the various software functions is shown in Fig. 4. In planning and executing scientific operations, the user can control 1) the command generator, which allows maneuvering from target to target as well as precision pointing during tracking or viewing inertial objects, 2) attitude updates that permit any combination of FGS, FHST, and gyro reference to be used for precision-pointing reference, 3) FGS acquisition of its guide stars, 4) control system gain selection, and 5) momentum management control. In addition to the pointing control functions, the operations user can also control the high-gain antennas and solar arrays. All of these elements work together to enable the HST PCS to perform precision pointing: the FGSs and gyros providing the attitude reference and rate data, the reaction wheels generating fine-control torques, and the flight software performing the PCS computations.

## Flight Hardware Improvements

The rate-integrating gyros selected for the HST have been employed in other spacecraft such as the High Energy Astronomy Observatory (HEAO) and the International Ultraviolet Explorer (IUE). In order to sense rates of milliarcsec/s, the gyro pulse weights were decreased to values cited previously and a dual-rate range was incorporated to provide the rate dynamic range. The stringent PCS requirements for the HST made performance upgrades of the sensors desirable. Several improvements were made to the gyros[4] based on an investigation undertaken to determine the major contributors to the gyro noise. The investigation resulted in several design improvements to reduce the noise characteristics.

The output power spectral density (PSD) for a gyro prior to noise reduction is shown in Fig. 5a. The noise at the output signal was traced to several sources. These sources were divided into two categories: mechanical and electrical noise. Major mechanical noise sources were due to gas flow characteristics around the gyro wheel and seismic disturbances at the test site. Electrical noise sources included wheel speed variations due to motor hunt, the coupling of various signals into the microsyn output, thermal noise from amplifier input, quantization errors, and grounding and shielding effects.

Initial attempts to reduce gyro noise focused on electrical sources. One approach to reducing the effect of this noise entailed reducing the electrical gain of the loop while maintaining the required overall loop gain. The redistribution of gains within the rate sensor was accomplished by a change in the fluid damping factor to increase the gyro gain, thereby allowing a reduction in electrical gain.

The wheel hunt contribution to the overall gyro noise is identified as the spike at 4.25 Hz in Fig. 5a. This effect was reduced with the addition of an antihunt circuit which uses a phase-locked loop. The resultant improvements in the gyro noise characteristics, as a result of the gain redistribution and antihunt circuit, is evident in Fig. 5b.

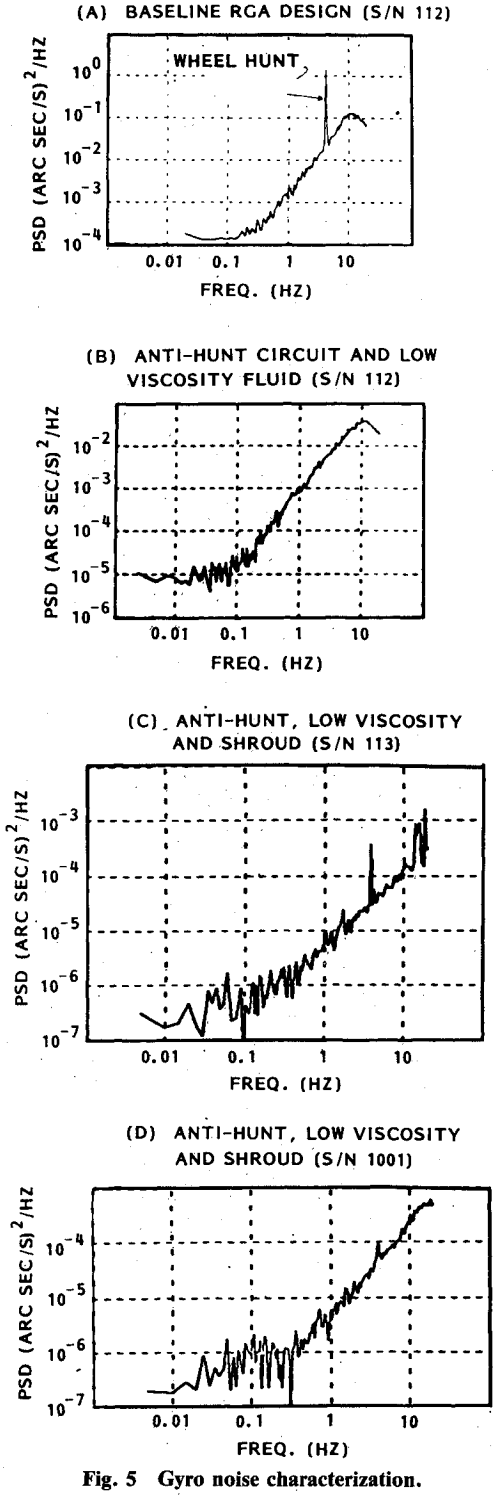


Fig. 5 Gyro noise characterization.

The final design modification was the result of an observed correlation between noise levels and wheel speed and the turbulence associated with the gyro wheel gas-bearing in the float. Analysis verified the existence of high turbulent flow within the float cavity. To correct this, a shroud was designed to restrict the gas flow around the wheel to the laminar region. The noise characteristics of the gyro following all three modifications are shown in Figs. 5c and 5d for the two design-proof test units.

The reaction wheels were also the subject of several upgrades. The wheel electrical noise was reduced during the initial design of the power bridges and motor drive circuits. The reaction wheels create harmonic forces which induce line-of-sight jitter. The stringent pointing requirements for the HST led to the need to reduce and isolate the induced vibration of the reaction wheels from the vehicle structural dynamics. The most significant disturbances in these low-noise wheels are the axial vibrations due to the imperfections of the bearings and their inner and outer raceways. This effect was minimized by carefully screening and matching the balls used in the bearings. To further attenuate reaction-wheel-induced vibration, isolators[5] were designed and installed on each of the reaction wheels, thereby improving the telescope's precision-pointing performance. The final design employs three pairs of fluid-damped isolator units per reaction wheel that attenuate vibrations above 18-20 Hz and place the isolator resonance frequencies near benign regions of structural dynamic response. The isolators were required to be stiff in torsion in order to be virtually transparent to the PCS.

These isolators were tested in the course of vehicle modal testing. The vehicle was suspended and floated on air bags while shakers excited the structure and accelerometers detected the structural response. During this period, a transfer function test was also run which applied torque to the reaction

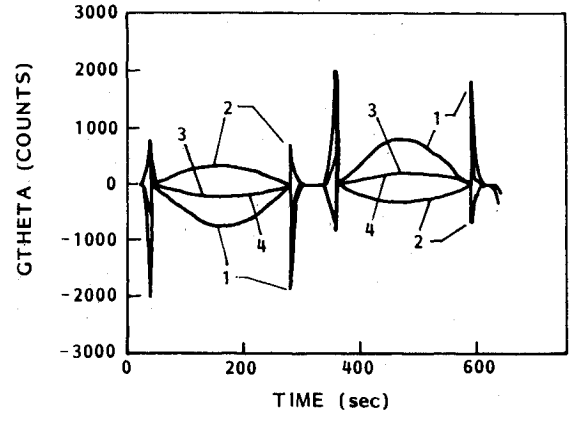


Fig. 6 Gyro pulse counts—engineering simulation.

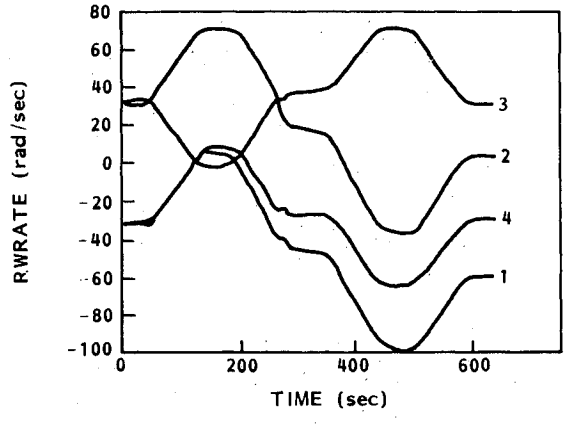


Fig. 7 Reaction wheel speeds—engineering simulation.

wheels and measured the response with the rate gyros and a precision angular displacement sensor. The signals from sensors and actuators were run through signal processing routines to obtain a transfer function for the structural response as seen by the PCS. The results compared well with a finite-element structural model and provided confidence that the reaction wheel performance is compatible with PCS requirements.

## Functional Testing

The precision-pointing performance requirements of the HST necessitated the establishment of a comprehensive test program. Testing was accomplished in three phases: 1) development testing, 2) hardware/software integration testing, and 3) HST assembly and verification. Each phase of testing used a common approach to allow continuity of the test comparison throughout the program. Development testing[6] was designed to validate engineering models and demonstrate interface compatibility. Hardware/software integration testing exercised HST PCS flight software in a flight data management system environment. Finally, HST vehicle test verification demonstrated the end item prior to launch.

Development testing was performed using rate gyros, reaction wheels, and a bread-board data management system on an air-bearing table. Closed-loop testing of the control system loop was made possible by the air-bearing table. This enabled the test bed to respond to reaction wheel torques, resulting in rotation rates that were then sensed by the gyros. In addition, a static test was run where the vehicle dynamics were modeled by an electronic PCS simulator that derived body rates based on the reaction wheel tachometer output and torqued the rate gyros accordingly. The simulator also had analog models of the gyros and reaction wheels so that identical test cases could be run using either the air-bearing table or the static simulation. The simulator incorporated a vehicle dynamics simulation and could use either the actual or simulated gyros and reaction wheels. The hardware models in the simulator were validated by comparing the results of the air-bearing and simulation tests. It was determined that the results were similar whether actual or simulated elements were being used.

Based on experience gained during development testing, the PCS simulator was improved for the vehicle system test. The simulator was rebuilt using a Digital Equipment Corp. PDP-11 to model the gyros, reaction wheels, FGSs, magnetic torquers, magnetometers, and coarse sun sensors. The PDP-11 interfaces with the HST data management system to exchange commands and data for each of the models. The selection between the hardware and simulation models is made via a command to the flight computer and does not involve any changes to the hardware configuration.

A Hardware/Software Integration Facility (HSIF) was established to perform the second phase of testing. This facility contains a PCS simulator and engineering model DF-224 flight computer and Data Management Unit. Although no PCS hardware is available in the hardware/software integration facility, most functions are modeled in the simulator to allow substantial testing of the flight software and its interfaces with the rest of the vehicle. Hardware/software integration testing has been so productive that the facility has been maintained to aid flight software development and checkout and to dry-run command loads to be used for the vehicle test. The HSIF will continue to be available following launch to support orbital operations.

Often the spacecraft test approach calls for testing various segments of a control system in an open-loop fashion. However, the uniqueness of the HST requirements motivated the decision to provide a means of testing the system with the control system loop closed. The PCS simulator provided that capability.

During vehicle testing, the extension from open-loop to closed-loop testing introduced a number of difficulties. The control loop is a high-gain system and can be torque-saturated by uncompensated biases and noise in the loop. In fine pointing, the rate gain is approximately 1.0 N-m/arcsec/s, resulting in loop saturation for rate errors above approximately 0.8 arcsec/s. After closing the loop, effects such as the Earth's rotation rate (15 arcsec/s) and gyro biases (up to 8 arcsec/s) become much more significant. The gyro biases being introduced into the system are measured off-line by accumulating raw gyro data from the telemetry stream in a decommutator and taking averages. The biases are then transformed into the spacecraft coordinate frame and loaded into the flight software to compensate the sensed body rates during testing.

In preparation for vehicle-level testing, a progressive series of pointing-control test cases was designed. Beginning with

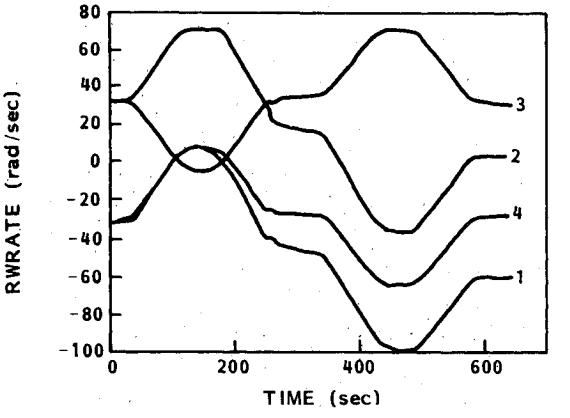


Fig. 9 Reaction wheel speeds—HSIF test.

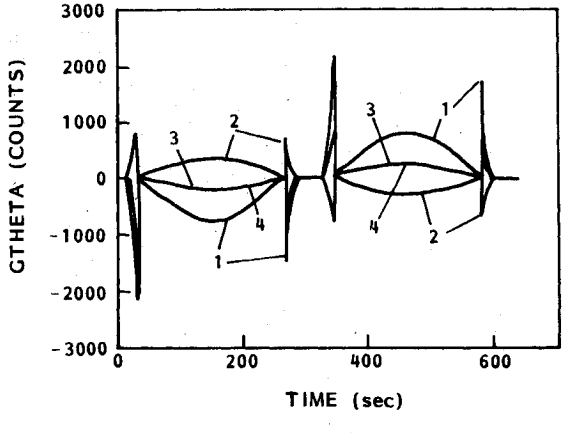


Fig. 8 Gyro pulse counts—HSIF test.

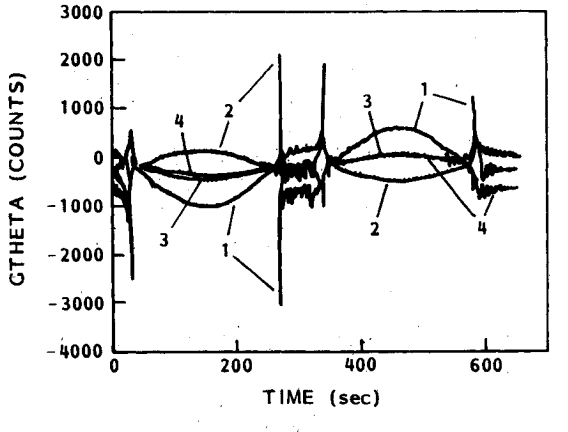


Fig. 10 Gyro pulse counts—system test.

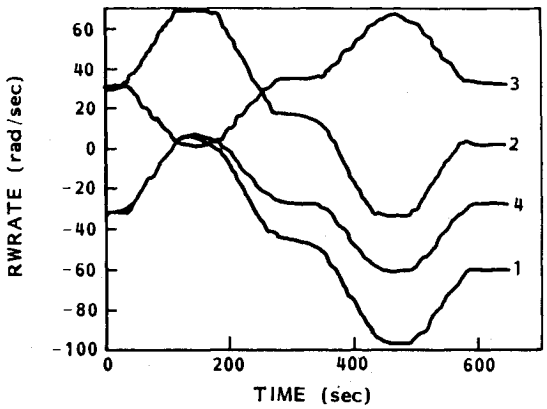


**Fig. 11 Reaction wheel speeds—system test.**

simple open-loop torque and rate steps, the cases increase in complexity to the point of doing multiple maneuvers while performing momentum management over several orbits. Mission-oriented tests were run, performing operational scenarios involving all subsystems and scientific instruments including vehicle and solar array slews, antenna tracking, star-tracker attitude updates, and scientific instrument data-taking.

A flight software/PCS-oriented computerized test system was developed to expedite the generation and analysis of test cases. This system produces a binary command load to be transmitted to the flight computer for the test execution and a set of plots of predicted results. The system begins with the preparation of an input file for executing an engineering functional simulation of the test scenario. The ouptut of the simulation can be plotted and used to predict the results of the test. A second simulation, which actually emulates the flight computer, can be run with the same input file with minor modifications. Among the outputs of this simulation is a file containing a flight computer command load that, when transmitted to the flight computer, will cause it to execute the scenario that was simulated. This command load can be run in the HSIF or on the actual vehicle. The telemetry from that execution can be plotted with the same scaling as the simulation output to allow side-by-side comparisons of test results vs predictions.

An example test case is illustrated in Figs. 6–11. A sequence of two maneuvers was commanded. The vehicle first slews 12 deg, and then back again, with a maximum rate of 250 arcsec/s on each maneuver. The rates on all three axes are equal. Figure 6 is the gyro rate profile on each of the four active gyros produced by the engineering simulation. The abrupt changes in the profile (e.g., at times of 40 and 280 s) occur as the body rates traverse a threshold that triggers a gyro-rate range mode switch. In low mode, a count corresponds to 0.005 arcsec/s, while a high-mode count is approximately equal to 0.3 arcsec/s. The reaction wheels from the same simulation are shown in Fig. 7. The wandering response is due to the simulated gravity gradient torques acting on the vehicle. A large number of other PCS-related plots are also generated automatically to allow a detailed analysis of the precision pointing.

A command load for this test case was generated, as described earlier, and run in the HSIF. Figures 8 and 9 were generated from HSIF data and exhibit close agreement with the predictions from the simulation. Figures 10 and 11 were plotted after the command load was run on the assembled vehicle. Again, the correlation is very good. Closer examination reveals a substantial amount of noise on the gyros, largely from air conditioners and the clean room filtration system. This noise is responsible for the choppy appearance of the wheel speed profiles in Fig. 11. In spite of the noise in the gyro signals, all test objectives were met and the functional ability of the PCS was demonstrated.

## Conclusion

Precision pointing is not easily demonstrated by one test. The ability to perform precision pointing is ensured by a combination of the hardware test data, the vehicle structural mode tests, the software demonstration in the HSIF, and the overall integration testing during vehicle system testing. The hardware test data on the FGSs, FHSTs, rate gyros, and reaction wheels demonstrate that each of the components can meet the allocated errors relative to the precision-pointing requirements. The integrated reaction wheel, rate gyro, and vehicle modal test setup demonstrated the ability to meet the structural interaction requirements. The HSIF provides visibility into the software computational errors and demonstrates that the software meets its precision-pointing requirements. The vehicle-level testing provides the overall confidence that the component parts of the precision-pointing system are working together and will provide the accuracy required.

## Acknowledgments

This work was sponsored by the NASA Marshall Space Flight Center, Huntsville, AL, under Contrct NAS8-32697. The authors wish to thank E. Moy for his assistance in executing the tests and preparing the data.

## References

[1]Dougherty, H. J., Tompetrini, K., Levinthal, J., and Nurre, G., "Space Telescope Observatory in Space," *Journal of Guidance, Control and Dynamics*, Vol. 5, July-Aug. 1982, p. 403.

[2]Dougherty, H. J. Rodoni, C., Rodden, J., and Tompetrini, K., "Space Telescope Pointing Control," *Astrodynamics 1983, Advances in the Astronautical Sciences,* Vols. 54 I & II, American Astronautical Society, 1983, pp. 619-630.

[3]Dougherty, H. J., Rossini, R., Simcox, D., and Bennett, N., "Space Telescope Control System Science User Operations," *Astrodynamics 1983, Advances in the Astronautical Sciences,* Vols. 54 I & II, American Astronautical Society, 1983, pp. 645-653.

[4]Rodden, J. et al., "Noise Performance Investigation and Improvement of a Rate Integrating Gyroscope," Eleventh Biennial Guidance Test Symposium, Holloman AFB, NM, 1983.

[5]Rodden, J. J., Dougherty, H. J., Reschke, L. F., Hasha, M. D., and Davis, L. P., "Line of Sight Performance Improvement with Reaction Wheel Isolation," American Astronautical Society Paper 86-005, Feb. 1986.

[6]Besonis, A., Dougherty, H. J., Nakashima, A., Tompetrini, K., and Meadows, P., "Development Testing for Space Telescope," IFAC Workshop, Stanford University, CA, Aug. 1983.